

Tetrameric $\alpha\beta\beta$ Aggregate Formation by Stereoisomeric Bidomain Helicene Oligomers**

Wataru Ichinose, Jun Ito, and Masahiko Yamaguchi*

Proteins form quaternary structures by the heteroaggregation of several subunits and exhibit functions as whole aggregates,^[1] which structurally can be dimeric, trimeric, tetrameric, and higher aggregates with various modes of homo- and heteroaggregation. Hemoglobin, which transports oxygen in red blood cells, forms a tetrameric $\alpha\beta\beta$ heteroaggregate from two α -subunits and two β -subunits, and exhibits physiologically important allosteric interactions between these subunits.^[2] Tetrameric $\alpha\beta\beta$ heteroaggregates were observed in coiled coil peptides^[3] and rigid-rod β -barrels,^[4] which are formed by peptide–peptide interactions. The aggregation was highly dependent on the amino acid residue.

From the enthalpic view, polymerized structures are favorable, because multiple aggregation gains a large free energy. It competes with the entropic effect, in which dimeric aggregates are most favorable, because the entropic loss is minimal. However, it may not be sufficient to explain tetrameric $\alpha\beta\beta$ aggregate formation simply by the balance of enthalpy and entropy, because such a balance most likely gives a complex mixture of aggregates. Specific tetrameric $\alpha\beta\beta$ heteroaggregate formation should include a concept not known at present. Thus, the development of a method of forming tetrameric $\alpha\beta\beta$ heteroaggregates using synthetic compounds is desirable to promote our understanding of protein functions and the development of novel drugs and biomaterials that interact with proteins.

In this study, we present a general method of specifically constructing $\alpha\beta\beta$ heteroaggregates without forming other homo- and heteroaggregates of dimeric, trimeric, pentameric, and polymeric structures. The method entails the aggregation of multidomain oligomers. Synthetic small-domain compounds^[5–8] and block copolymers^[9] form polymeric heteroaggregates; however, the formation of specific higher aggregates such as the $\alpha\beta\beta$ tetrameric heteroaggregate is not yet known.

We have recently reported the dimeric homoaggregate formation of the bidomain oligomer $(P)\text{-A4}(P)\text{-E7}$,^[10] which

contained the (P) -amidohelicene^[11] tetramer domain $(P)\text{-A4}$ and the (P) -ethynylhelicene^[12] heptamer domain $(P)\text{-E7}$, and dimeric heteroaggregate formation of the tridomain oligomers $(P)\text{-A4}(P)\text{-E5}(P)\text{-A4}$ and $(P)\text{-A4}(M)\text{-E5}(P)\text{-A4}$.^[13] Herein, bidomain oligomers $(M)\text{-A4}(M/P)\text{-E5}$ were used for tetrameric $\alpha\beta\beta$ heteroaggregate formation. The method exploits the different stabilities of the homo- and heteroaggregates at the amido tetramer domain $(M)\text{-A4}$ and the ethynyl pentamer domains $(M/P)\text{-E5}$ (Figure 1). The stabil-

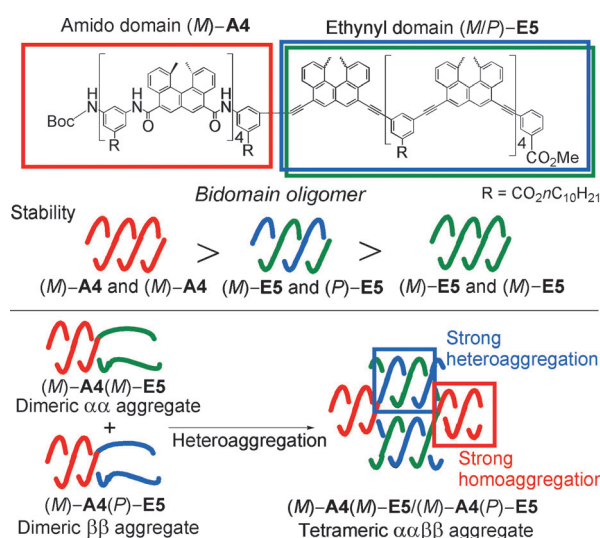


Figure 1. Tetrameric $\alpha\beta\beta$ aggregate formation by stereoisomeric bidomain oligomers.

ities are in the order: $(M)\text{-A4}$ and $(M)\text{-A4} > (M)\text{-E5}$ and $(P)\text{-E5} > (M)\text{-E5}$ and $(M)\text{-E5}$. The homoaggregation of $(M)\text{-A4}$ is much stronger than that of $(M)\text{-E5}$, and the heteroaggregation of $(M)\text{-E5}$ and $(P)\text{-E5}$ is much stronger than the homoaggregation.^[14] Also, no aggregation occurs between the amido domain $(M)\text{-A4}$ and the ethynyl domain $(M/P)\text{-E5}$. Otherwise, complex mixtures of aggregates would form.

With regards to solvent effects, it is known that the amido domain in $(P)\text{-A4}(P)\text{-E7}$ forms dimeric aggregates in chloroform, and disaggregates in THF; chloroform, chlorobenzene, and toluene are solvents that moderately promote double-helix formation at the ethynyl domain, and THF induces disaggregation.^[10–12]

A two-step manipulation method was employed to obtain a tetrameric $\alpha\beta\beta$ aggregate, which entailed the preparation of separate solutions of the bidomain oligomers $(M)\text{-A4}(M)\text{-E5}$ (α -subunit) and $(M)\text{-A4}(P)\text{-E5}$ (β -subunit) in the dimeric $\alpha\alpha$ and $\beta\beta$ homoaggregated states, and the mixing of the

[*] Dr. W. Ichinose, J. Ito, Prof. Dr. M. Yamaguchi
Department of Organic Chemistry, Graduate School of Pharmaceutical Sciences, Tohoku University
Aoba, Sendai 980-8578 (Japan)
E-mail: yama@mail.pharm.tohoku.ac.jp
Homepage: <http://www.pharm.tohoku.ac.jp/~sekkei/yakan-home.html>

[**] This work was financially supported by a Grant-in-Aid for Scientific Research (21229001).

Supporting information for this article is available on the WWW under <http://dx.doi.org/10.1002/anie.201301463>.

solutions. The amido domain (*M*)-**A4** remains aggregated during manipulation, and the heteroaggregation of the ethynyl domains (*M*)-**E5** and (*P*)-**E5** predominate over homoaggregation, giving the desired tetrameric $\alpha\beta\beta$ heteroaggregate without forming other lower or higher aggregates. The tetrameric $\alpha\beta\beta$ heteroaggregate transformed into dimeric $\alpha\alpha$ and $\beta\beta$ aggregates, random coils of α/β -subunits, and polymeric $(\alpha\beta\beta)_n$ aggregates, depending on the environment.

The bidomain oligomers (*M*)-**A4**(*M*)-**E5** and (*M*)-**A4**(*P*)-**E5** were synthesized and shown to form four states: all dimer, amido dimer, ethynyl dimer, and random coil, which is similar to related bidomain oligomers (Figure S1 and S2).^[10] For example, the all-dimer state is aggregated at both the amido and ethynyl domains, and the amido-dimer state is aggregated at the amido domain, but not at the ethynyl domain. Chloroform solutions (1×10^{-4} M) of (*M*)-**A4**(*M*)-**E5** and (*M*)-**A4**(*P*)-**E5** were prepared, the circular dichroism (CD) analysis of which indicated that (*M*)-**A4**(*M*)-**E5** was an 8:2 mixture of the amido dimer and all dimer (Figure S3a), and that (*M*)-**A4**(*P*)-**E5** was an amido dimer (Figure S3b). Then, the solutions were mixed in a 1:1 ratio and allowed to settle for 1 h at room temperature. The UV/Vis spectrum of the (*M*)-**A4**(*M*)-**E5**/*M*)-**A4**(*P*)-**E5** mixture was different from the calculated spectrum obtained by adding the spectrum of each oligomer in the same solvent, and from the calculated spectrum obtained by adding the spectrum of each oligomer in the random coil state. The increase in the absorbance at 340–380 nm and the decrease at 300–340 nm are consistent with heteroaggregation at the ethynyl domain (Figure 2a).^[14] The CD spectrum of the mixture was also different from the calculated spectra (Figure 2b). The Job plot experiment using the UV absorption at 364 nm in chloroform revealed complex formation in a 1:1 ratio (Figure 3). The amido domain does not disaggregate in chloroform.^[11] Then, the aggregate formation of (*M*)-**A4**(*M*)-**E5** and (*M*)-**A4**(*P*)-**E5** was considered to occur by homoaggregation at the amido domain and heteroaggregation at the ethynyl domain.

The (*M*)-**A4**(*M*)-**E5**/*M*)-**A4**(*P*)-**E5** mixture in chloroform (1×10^{-4} M) was analyzed by gel permeation chromatography (GPC), which exhibited a peak with a retention time of 11.5 min accompanied by a very small peak at 12.6 min (Figure 4a). The latter peak coincided with those of (*M*)-**A4**(*M*)-**E5** and (*M*)-**A4**(*P*)-**E5** (Figure 4c,d, respectively). The co-injection of the (*M*)-**A4**(*M*)-**E5**/*M*)-**A4**(*P*)-**E5** mixture and (*M*)-**A4**(*M*)-**E5** showed two peaks at 11.5 and 12.6 min (Figure 4b). The peak at 11.5 min was assigned to an aggregate higher than a dimer. The same experiment at 1×10^{-3} M gave a similar HPLC result (Figure S4), and vapor pressure osmometry (VPO) analysis (1×10^{-3} M, 35 °C, chloroform) provided an apparent molecular weight of 2.2×10^4 , which coincided with the calculated value (21,871) obtained from two (*M*)-**A4**(*M*)-**E5** oligomers and two (*M*)-**A4**(*P*)-**E5** oligomers. The result was compared with the apparent molecular weights of the homoaggregated (*M*)-**A4**(*M*)-**E5** and (*M*)-**A4**(*P*)-**E5**, both 1.1×10^4 , as determined by VPO (1×10^{-3} M, 35 °C, chloroform). Dynamic light scattering (DLS) analysis (chloroform) of the (*M*)-**A4**(*M*)-**E5**/*M*)-**A4**(*P*)-**E5** mixture showed the formation of particles of a 40 nm average

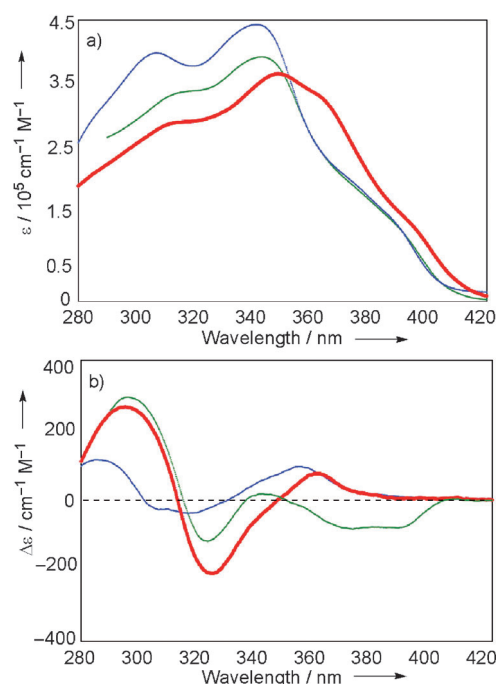


Figure 2. UV/Vis spectrum (a) and CD spectrum (b) of an (*M*)-**A4**(*M*)-**E5**/*M*)-**A4**(*P*)-**E5** mixture (chloroform, 1×10^{-4} M, 25 °C; red line). The calculated CD and UV/Vis spectra were obtained by adding the spectra of (*M*)-**A4**(*M*)-**E5** and (*M*)-**A4**(*P*)-**E5** (chloroform, 1×10^{-4} M, 25 °C; green line). The calculated spectra of the random coils were obtained by adding the spectra of (*M*)-**A4**(*M*)-**E5** and (*M*)-**A4**(*P*)-**E5** (THF, 2.5×10^{-6} M, 25 °C; blue line).

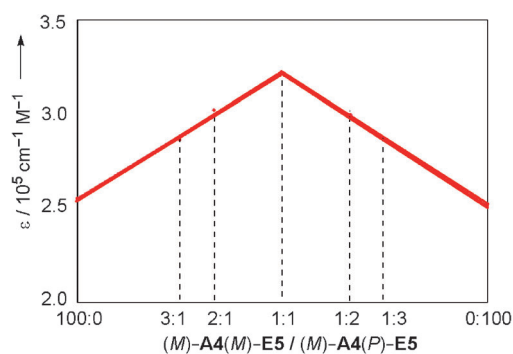


Figure 3. Job plot experiment (chloroform, 1×10^{-4} M, 25 °C) using ϵ (364 nm) against (*M*)-**A4**(*M*)-**E5**/*M*)-**A4**(*P*)-**E5** ratio.

diameter, which was larger than the homoaggregates of (*M*)-**A4**(*M*)-**E5** and (*M*)-**A4**(*P*)-**E5** (7 nm average diameter; Figure 5). Atomic force microscopy (AFM) images of the sample prepared from the (*M*)-**A4**(*M*)-**E5**/*M*)-**A4**(*P*)-**E5** mixture showed dispersed particles of 45 nm diameter (Figure S5), which is in good agreement with the results of the DLS analysis. The experiments indicated specific formation of the tetrameric $\alpha\beta\beta$ aggregate without the formation of other lower and higher aggregates, and showed the validity of the method noted in the introduction.

The interconversion between the tetrameric $\alpha\beta\beta$ heteroaggregate and the dimeric $\alpha\alpha$ and $\beta\beta$ homoaggregates was examined. In chloroform, heating the (*M*)-**A4**(*M*)-**E5**/*M*)-

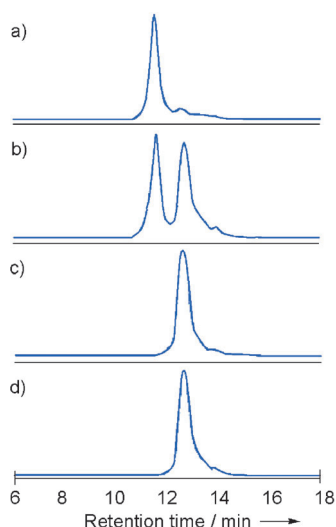


Figure 4. HPLC profile (chloroform, 1×10^{-4} M, RT) of a) the (M)-A4(M)-E5/(M)-A4(P)-E5 mixture, b) co-injection of the (M)-A4(M)-E5/(M)-A4(P)-E5 mixture and (M)-A4(M)-E5, (c) (M)-A4(M)-E5, (d) (M)-A4(P)-E5. Chloroform mobile phase, flow rate = 0.5 mL min^{-1} , $\lambda = 290 \text{ nm}$, $7.5 \times 300 \text{ mm}$ MesoPore column.

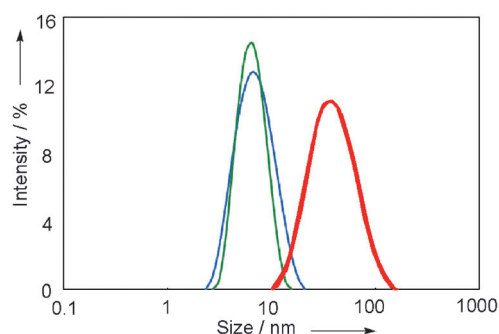


Figure 5. Size distributions of the (M)-A4(M)-E5/(M)-A4(P)-E5 mixture determined by DLS analysis in chloroform (1×10^{-4} M, 20°C ; red line). Those of the homomeric aggregates of (M)-A4(M)-E5 (green line) and (M)-A4(P)-E5 (blue line) in chloroform (1×10^{-4} M, 20°C) are also shown.

A4(P)-E5 (1×10^{-4} M) mixture at 60°C did not change the UV/Vis spectra (Figure S6), which indicated a strong tetrameric aggregation under the conditions used. Then, the solvent was changed to chlorobenzene to slightly weaken the aggregation. The (M)-A4(M)-E5/(M)-A4(P)-E5 mixture in chlorobenzene at 20°C formed the tetrameric $\alpha\alpha\beta\beta$ aggregate, which showed the same CD, UV/Vis, and HPLC profiles as that in chloroform (Figure S7 and S8). When the mixture was heated at 90°C for 20 min, UV/Vis absorbance at 360 nm decreased, and the resulting spectrum coincided with the calculated spectrum obtained by adding the spectra of (M)-A4(M)-E5 and (M)-A4(P)-E5 at the same temperature in the dimeric $\alpha\alpha$ and $\beta\beta$ aggregate forms (Figure 6a). DLS analysis (chlorobenzene, 90°C) of the (M)-A4(M)-E5/(M)-A4(P)-E5 mixture showed a main peak for the $\alpha\alpha/\beta\beta$ aggregates of 7 nm average diameter and a minor at 40 nm for the $\alpha\alpha\beta\beta$ aggregate (Figure S9). The heating-cooling cycle at 20 and 90°C was repeated, and the $\Delta\epsilon(364 \text{ nm})/\text{time}$ profiles were obtained in a reproducible manner (Figure 6b). The tetra-

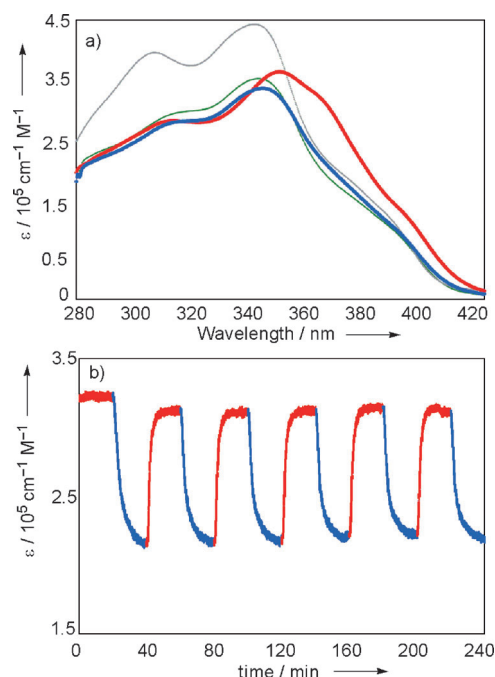


Figure 6. (a) UV/Vis spectra of the (M)-A4(M)-E5/(M)-A4(P)-E5 mixture (chlorobenzene, 1×10^{-4} M) at 20°C (red line) and 90°C (blue line). The calculated UV/Vis spectrum obtained by adding the spectra of homomeric aggregates of (M)-A4(M)-E5 and (M)-A4(P)-E5 (chlorobenzene, 1×10^{-4} M, 90°C ; green line) is shown. The calculated UV/Vis spectrum of the random coils (THF, 2.5×10^{-6} M, 25°C ; gray line) is also shown. (b) ϵ -Time profiles using ϵ values at 364 nm of the (M)-A4(M)-E5/(M)-A4(P)-E5 mixture (chlorobenzene, 1×10^{-4} M) in repeating cycles of $90/20^\circ\text{C}$ every 20 min.

meric $\alpha\alpha\beta\beta$ heteroaggregate reversibly changed its structure between the dimeric $\alpha\alpha$ and $\beta\beta$ homomeric aggregates on heating and cooling (Figure 7).

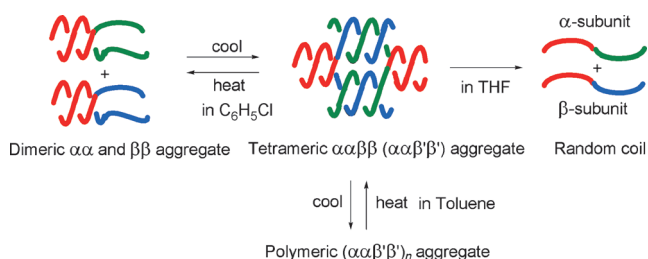


Figure 7. Structure change of tetrameric $\alpha\alpha\beta\beta$ heteroaggregates of (M)-A4(M)-E5/(M)-A4(P)-E5.

The tetrameric $\alpha\alpha\beta\beta$ aggregate was converted into random coils by adding THF. A chloroform solution (1×10^{-4} M) of (M)-A4(M)-E5/(M)-A4(P)-E5 in the tetrameric $\alpha\alpha\beta\beta$ aggregate state was prepared, and THF was added to make a solution of 10% chloroform in THF (1×10^{-5} M). The CD and UV/Vis spectra were in good agreement with the calculated spectra of the random coils (Figure S10). The GPC analysis in 10% chloroform/THF showed a peak at 13.8 min, which was assigned to the random coils of (M)-A4(M)-E5 and (M)-A4(P)-E5 (Figure S11).

Another combination of the oligomers (*M*)-**A4**(*M*)-**E5** (α -subunit) and (*M*)-**A4**(*P*)-**E4** (β' -subunit) was examined, where (*M*)-**A4**(*P*)-**E4** instead of (*M*)-**A4**(*P*)-**E5** (β -subunit) was used to slightly suppress heteroaggregation at the ethynyl domain. The oligomer (*M*)-**A4**(*P*)-**E4** in chloroform (1×10^{-4} M), which gave the amido-dimer state (Figure S1c), was mixed with (*M*)-**A4**(*M*)-**E5** in chloroform (1×10^{-4} M) in a 1:1 ratio. The CD and UV/Vis spectra of the (*M*)-**A4**(*M*)-**E5**/*M*)-**A4**(*P*)-**E4** mixture were similar to those of (*M*)-**A4**(*M*)-**E5**/*M*)-**A4**(*P*)-**E5** (Figure S12). The GPC analysis in chloroform showed two peaks at 11.5 min and 12.6 min in a 1:1 area ratio (Figure S13), which indicated the formation of a 1:1 mixture of the tetrameric $\alpha\beta\beta'$ aggregate and the dimeric $\alpha\alpha$ and $\beta'\beta'$ aggregates. VPO analysis (chloroform, 35 °C) provided apparent molecular weights of 1.5×10^4 (1×10^{-3} M) and 1.6×10^4 (2×10^{-3} M), which is consistent with the formation of a 1:1 mixture. The tetrameric $\alpha\beta\beta'$ aggregate was formed in the (*M*)-**A4**(*M*)-**E5**/*M*)-**A4**(*P*)-**E4** system.

Pseudoenantiomeric ethynylhelicene oligomers form two-component gels by intercomplex interactions between hetero-double helices.^[14,15] In this study, a gel formed for the tetrameric $\alpha\beta\beta'$ aggregate of the (*M*)-**A4**(*M*)-**E5**/*M*)-**A4**(*P*)-**E4** mixture in toluene. Solutions of (*M*)-**A4**(*M*)-**E5** and (*M*)-**A4**(*P*)-**E4** in toluene (6×10^{-3} M) were prepared and mixed in a 1:1 v/v ratio. A gel that did not flow when its containing flask was turned upside down was formed after leaving the mixture at room temperature for 1 h (Figure 8). A

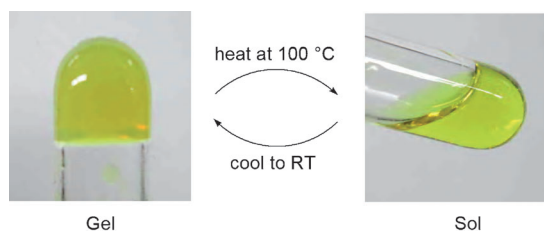


Figure 8. Photographs of (*M*)-**A4**(*M*)-**E5**/*M*)-**A4**(*P*)-**E4** in the gel form (left) and sol form (right) in toluene (6×10^{-3} M).

minimum gelation concentration (MGC) of 6×10^{-3} M was determined by varying the concentration. AFM analysis of the gel showed a fiber network structure of 100 nm diameter (Figure S14). The gel (6×10^{-3} M) interconverted between sol and gel by heating at 100 °C and cooling to room temperature. The CD and UV/Vis spectra (1×10^{-3} M) of the gel were similar in shape to those of the tetrameric $\alpha\beta\beta'$ aggregate of (*M*)-**A4**(*M*)-**E5**/*M*)-**A4**(*P*)-**E5** (Figure S15).

It was confirmed that the tetrameric $\alpha\beta\beta'$ heteroaggregate was formed in toluene at a low concentration (5×10^{-5} M). The CD and UV/Vis spectra (5×10^{-5} M, 25 °C, toluene) of the (*M*)-**A4**(*M*)-**E5**/*M*)-**A4**(*P*)-**E4** mixture in the sol state were similar to those of the gel (1×10^{-3} M; Figure S15). DLS and AFM analysis showed the formation of particles of a 45–50 nm average diameter (Figure S16 and S17). These results indicated that the tetrameric $\alpha\beta\beta'$ aggregate is formed at low concentrations in toluene, and that gels are formed at high concentrations by the formation of polymeric $(\alpha\beta\beta')_n$

aggregates. This is a notable example of a four-component gel formed by molecular self-assembly.

In summary, a method of forming a tetrameric $\alpha\beta\beta'$ heteroaggregate has been developed using two bidomain oligomers for the α - and β -subunits, which possess a domain with a very strong ability to form homoaggregates and another domain with a strong ability to form heteroaggregates. Mixing the dimeric $\alpha\alpha$ and $\beta\beta$ homoaggregates gave tetrameric $\alpha\beta\beta'$ heteroaggregates without forming higher and lower aggregates. The tetrameric $\alpha\beta\beta'$ heteroaggregates exhibited structural changes like those of proteins: 1) reversible structural change to form the dimeric $\alpha\alpha$ and $\beta\beta$ homoaggregates by disaggregation at the ethynyl domain; 2) disaggregation to form random coils; and 3) reversible polymerization and gel transition. The multidomain oligomer method developed may be used for the formation of various specific higher heteroaggregates.

Received: February 19, 2013

Published online: April 9, 2013

Keywords: gels · helical structures · heteroaggregate · structure change · tetrameric

- [1] G. A. Petsko, *Protein Structure and Function*, New Science, London, **2004**.
- [2] A. M. Lesk, *Introduction to Protein Science Architecture, Function & Genomics*, Oxford University Press, Oxford, **2004**.
- [3] a) R. Fairman, H.-G. Chao, T. B. Lavoie, J. J. Villafranca, G. R. Matsueda, J. Novotny, *Biochemistry* **1996**, *35*, 2824–2829; b) J. L. Price, W. S. Horne, S. H. Gellman, *J. Am. Chem. Soc.* **2007**, *129*, 6376–6377; c) B. C. Root, L. D. Pellegrino, E. D. Crawford, B. Kokona, R. Fairman, *Protein Sci.* **2009**, *18*, 329–336.
- [4] a) B. Baumeister, S. Matile, *Chem. Eur. J.* **2000**, *6*, 1739–1749; b) B. Baumeister, S. Matile, *Chem. Commun.* **2000**, 913–914; c) G. Das, S. Matile, *Chirality* **2001**, *13*, 170–176.
- [5] For reviews of heteroaggregation by small organic molecules, see: M. M. Safont-Sempere, G. Fernández, F. Würthner, *Chem. Rev.* **2011**, *111*, 5784–5814.
- [6] For examples of polymeric heteroaggregates, see: a) T. Park, S. C. Zimmerman, *J. Am. Chem. Soc.* **2006**, *128*, 13986–13987; b) F. Wang, C. Han, C. He, Q. Zhou, J. Zhang, C. Wang, N. Li, F. Huang, *J. Am. Chem. Soc.* **2008**, *130*, 11254–11255; c) N. Tomimatsu, A. Kanaya, Y. Takashima, H. Yamaguchi, A. Harada, *J. Am. Chem. Soc.* **2009**, *131*, 12339–12343.
- [7] For examples of dimeric heteroaggregates, see: a) H. Ito, Y. Furusho, T. Hasegawa, E. Yashima, *J. Am. Chem. Soc.* **2008**, *130*, 14008–14015; b) Q. Gan, F. Li, G. Li, B. Kauffmann, J. Xiang, I. Huc, H. Jiang, *Chem. Commun.* **2010**, *46*, 297–299; c) H.-B. Wang, B. P. Mudraboyina, J. A. Wisner, *Chem. Eur. J.* **2012**, *18*, 1322–1327.
- [8] For examples of oligomeric heteroaggregates by Vernier assembly, see: a) C. A. Hunter, S. Tomas, *J. Am. Chem. Soc.* **2006**, *128*, 8975–8979; b) C. A. Hunter, *Nature* **2011**, *469*, 39–41.
- [9] a) C. Hiemstra, Z. Zhong, L. Li, J. P. Dijkstra, J. Feijen, *Biomacromolecules* **2006**, *7*, 2790–2795; b) H. R. Marsden, A. V. Korobko, E. N. M. Van Leeuwen, E. M. Pouget, S. J. Veen, N. A. J. M. Sommerdijk, A. Kros, *J. Am. Chem. Soc.* **2008**, *130*, 9386–9393; c) C. Tang, E. M. Lennon, G. H. Fredrickson, E. J. Kramer, C. J. Hawker, *Science* **2008**, *322*, 429–432.

- [10] W. Ichinose, M. Shigeno, M. Yamaguchi, *Chem. Eur. J.* **2012**, *18*, 12644–12654.
- [11] R. Amemiya, W. Ichinose, M. Yamaguchi, *Bull. Chem. Soc. Jpn.* **2010**, *83*, 809–815.
- [12] a) H. Sugiura, Y. Nigorikawa, Y. Saiki, K. Nakamura, M. Yamaguchi, *J. Am. Chem. Soc.* **2004**, *126*, 14858–14864; b) H. Sugiura, M. Yamaguchi, *Chem. Lett.* **2007**, *36*, 58–59; c) H. Sugiura, R. Amemiya, M. Yamaguchi, *Chem. Asian J.* **2008**, *3*, 244–260; d) R. Amemiya, N. Saito, M. Yamaguchi, *J. Org. Chem.* **2008**, *73*, 7137–7144; e) K. Yamamoto, H. Sugiura, R. Amemiya, H. Aikawa, Z. An, M. Yamaguchi, M. Mizukami, K. Kurihara, *Tetrahedron* **2011**, *67*, 5972–5978.
- [13] W. Ichinose, J. Ito, M. Yamaguchi, *J. Org. Chem.* **2012**, *77*, 10655–10667.
- [14] N. Saito, M. Shigeno, M. Yamaguchi, *Chem. Eur. J.* **2012**, *18*, 8994–9004.
- [15] a) R. Amemiya, M. Mizutani, M. Yamaguchi, *Angew. Chem.* **2010**, *122*, 2039–2043; *Angew. Chem. Int. Ed.* **2010**, *49*, 1995–1999; b) K. Yamamoto, N. Oyamada, M. Mizutani, Z. An, N. Saito, M. Yamaguchi, M. Kasuya, K. Kurihara, *Langmuir* **2012**, *28*, 11939–11947.
-